Communications on Applied Nonlinear Analysis
ISSN: 1074-133X
Vol 32 No. 1 (2025)

Enhancing Bright Band Prediction Through RadioSonde RadioWind for International Telecommunication Union- Radio Communications (ITU-R)

1st Likhitha Banredddy, 1st Krishna Reddy Maddikera, 2nd Dr B Ravi Chandra, 3rd Lokanath Reddy Maddikera, 4th Krishnaveni Sodum

[1,2]Department of Electronics and Communication Engineering, G.Pullaiah College of Engineering and Technology Kurnool, Andhra Pradesh, India; [3]Department of Civil Engineering, G.Pullaiah College of Engineering and Technology Kurnool, Andhra Pradesh, India; [4]Department of Physics, Sri Chaitanya Junior College, Kurnool, Andhra Pradesh,India.
likhithareddy278@gmail.com, krishnareddymaddikeras@gmail.com

Article History:

Received: *13-07-2024*

Revised: *29-08-2024*

Accepted: *10-09-2024*

Abstract

As a vital source of information on atmospheric conditions at different altitudes, upper air observations are critical for precise weather forecasting, climate monitoring, and atmospheric research. In coastal areas like Vishakhapatnam that are subject to tropical cyclones and monsoonal fluctuations, radiosondes provide precise vertical profiles that are essential for weather forecasting. They also measure temperature, humidity, and pressure. The addition of wind speed and direction readings via radiowind devices, often known as "rawinsondes," improves severe weather forecasts and our understanding of atmospheric dynamics. Forecasting floods, maintaining aviation safety, and managing water resources are all aided by the ability to predict the bright band, a radar indication of the precipitation layer melting. Weather models and readiness for disasters are much improved in Vishakhapatnam when radiosondes, rawinsondes, and bright band predictions are used in tandem.

Keywords: upper air observations, radiosondes, rawinsondes, RadioWind systems, bright band, precipitation estimates, flood forecasting, water resource management and disaster preparedness.

1. Introduction

With an emphasis on Burkina Faso, Ghana, and Senegal, the International Telecommunications Union (ITU) launched the "Radio Wave Propagation Measurement Campaign for Africa" in 1984. The campaign found that low humidity, radiative cooling, and super-refractive propagation circumstances were the causes of signal fading. To improve radio propagation models in Botswana and bring them into compliance with ITU-R standards, the study recommends improved data collecting and ongoing measurement initiatives. Radiosonde launches and data retrieval are facilitated by the Department of Meteorological Services [1]. From December 13 to December 15, 2018, a mid-level supercooled liquid cloud layer with a cloud top at 3500 meters and a thickness of 700 meters was observed over south and central China. For the first seven hours, water droplets the size of drizzles were visible beneath the cloud, according to lidar data collected from above. Significant wind shear, a high relative humidity, and a warm front were all present in this layer. It was revealed by satellite data and ECMWF reanalysis that a tropical storm in the Bay of Bengal was responsible for the moisture transport from the Indian Ocean. Research on the creation and durability of these kinds of clouds is still needed, as the study made clear [2]. This paper proposes a procedure for creating climatological limit thresholds for temperature and wind data obtained from high-resolution radiosondes. Applying objective criteria, the approach finds errors using percentile profiles (PPs) from 64 vertical bins. The efficiency of the strategy is confirmed by field data collected in the Tibetan Plateau. By providing an intuitive evaluation of departures from typical ranges, the thresholds aid in the identification of gross errors. In data from 123 Chinese upper-air monitoring sites, the effectiveness of the system in quality control is illustrated [3]. The recovery of water vapor profiles from simulated Suomi NPP CrIS hyperspectral pictures is discussed, as well as the practical limitations of remote sensing inverse problems. It highlights the superiority of deterministic regularized total least squares (RTLS) method in finding unique solutions by contrasting it with a stochastic approach. RTLS does not rely on apriori error covariance matrices; instead, it use data-driven regularization to stop noise enhancement. The research explores the limitations and complexities of the stochastic method and regularization strategies while showcasing the promise of RTLS in satellite inversion. The effectiveness of the RTLS technique in enhancing water vapor profile recovery is confirmed by simulated retrievals [4]. For GNSS-IR, the Novel Interferometric Tropospheric Error (NITE), this includes geometric displacement error, route delay, and bending angle correction. NITE provides increased accuracy for tropospheric correction in GNSS-IR sea level monitoring, as demonstrated by its validation using raytracing and radiosonde data. The study demonstrates the superior performance of NITE in long-term sea-level retrievals, while also highlighting the limitations and severe elevation-dependent biases of existing approaches. The technique uses trigonometric principles to connect reflector height to interferometric radio length, and the geometric displacement error is negligible. The results highlight NITE's ability to improve GNSS-IR's accuracy in sea level monitoring [5]. Using GNSS Radio Occultation (RO), this study investigates the temporal and spatial variability of precipitable water vapor (PWV) in Egypt from 2006 to 2021. PWV has a negative relationship with latitude; it is higher near the Mediterranean coast and at lower latitudes. The annual PWV has a range of 9.23 mm to 13.51 mm, with summer and daytime readings being greater. Reliability of the RO approach was confirmed by the low bias it displayed when compared to radiosonde data. The study's conclusions contribute to our knowledge of atmospheric water vapor's function in climate and weather patterns as well as high-resolution weather forecasting [6]. The study examines changes in temperature, pressure, and water vapor pressure (WVP) by comparing GPS radio occultation (RO) and radiosonde (RS) atmospheric profiles collected over a ten-year period in Egypt. At higher elevations, there were significant fluctuations in temperature and pressure, and significant differences in WVP that affected refraction levels. With the exception of WVP, the research verifies the integration of RO and RS data, demonstrating strong correlation (≥0.99) between profiles. The good alignment of RO and RS data, in spite of temporal and spatial disparities, supports the combined use of these data sources for precise atmospheric monitoring in Egypt [7]. In a thirteen-month investigation, RMIT University used data from 35 Australian and Antarctic radiosonde stations to examine air characteristics from COSMIC GPS radio occultation (RO). Strong agreement was seen, particularly in arid regions, between COSMIC profiles and radiosonde observations, with little variations in pressure and temperature. High-precision, all-weather upper-air data from the COSMIC RO data set is essential for Australian meteorological research. There is a lot of promise for weather and climate studies because this technology is integrated into Australia's forecasting system. In Australia, joint efforts are being made to optimize the advantages of GNSS RO technology [8]. Boundary layer heights (BLH) measured using radiosondes and microwave radiometers (MWR) at Beijing Southern Meteorological Observatory between April 2017 and March 2018 are compared in this study. The findings indicate that BLH calculated from MWR is, on average, 157 meters higher than BLH generated from radiosonde data, with the least differences found between 08:00 and 20:00 BJT and in the spring and summer. Beijing's BLH is lower at night, averaging about 622 meters. The work emphasizes how crucial BLH is to comprehending turbulence and pollution spread in climate models. Subsequent investigations ought to concentrate on enhancing Bayesian least square estimates and investigating diverse methods in diverse stable scenarios [9]. A comparison of 11-year planetary boundary layer height (PBLH) data from the Integrated Global Radiosonde Archive (IGRA), COSMIC soundings, and ERA-Interim reanalysis is presented. Results indicate that between 1200 and 0000 UTC, ERA-Interim and IGRA generally agree, with noon PBLH values being particularly high because of convective activity. When comparing the three datasets, COSMIC PBLHs are much greater at low latitudes and lower at high latitudes than those from radiosonde and reanalysis data. Wintertime sees larger seasonal differences, while summertime sees smaller ones. Predicting weather, climate change, and air quality all depend on accurate PBLH estimation [10]. Radiosondes are vital meteorological instruments in India, providing upper air data necessary for precise weather forecasting, climate monitoring, and atmospheric research. A radiosonde is a battery-operated sensor package that measures different atmospheric characteristics at different altitudes, usually carried into the atmosphere by a weather balloon. Then, real-time transmission of this data is made to receiving stations situated on the ground. Radiosonde deployment and administration are supervised by the India Meteorological Department (IMD) throughout the nation. The IMD was founded in 1875 and is the principal organization in India for seismology, weather forecasting, and meteorological measurements. As a component of a larger observational network that encompasses surface and upper air observations, the IMD runs a network of radiosonde stations [11,12]. Because of India's varied and complicated climate, radiosondes are extremely important there. A variety of weather phenomena, such as the monsoon, tropical cyclones, and intense thunderstorms, can be better understood and predicted with the use of radiosonde data. India's agricultural and water supplies depend on the monsoon, which is influenced by a number of atmospheric processes that are better understood through upper air measurements. The capabilities of radiosondes utilized in India have improved due to technological improvements. In addition to standard temperature, humidity, and pressure readings, modern radiosondes are furnished with GPS receivers to yield precise wind speed and direction data. Understanding the atmospheric dynamics over the Indian subcontinent is aided by this additional data, which greatly increases the accuracy of weather forecasts [13,14]. Particularly useful are radiosonde observations in coastal areas such as Vishakhapatnam. Vishakhapatnam is subject to notable monsoonal fluctuations and is vulnerable to tropical cyclones. The region's radiosonde data is useful for tracking and forecasting these occurrences, which can have a significant impact on the local climate and weather as well as the population's safety and way of life. Radiosondes are an essential component of India's meteorological observations, providing crucial information for climate research and weather forecasting. The IMD's deployment of them guarantees thorough monitoring of the upper atmosphere, improving our comprehension of India's intricate weather processes [14].

2. Objectives

To find the Bright Band or Melting Layer Height for ITU-R applicable for Wireless Communication Systems.

3. Methods

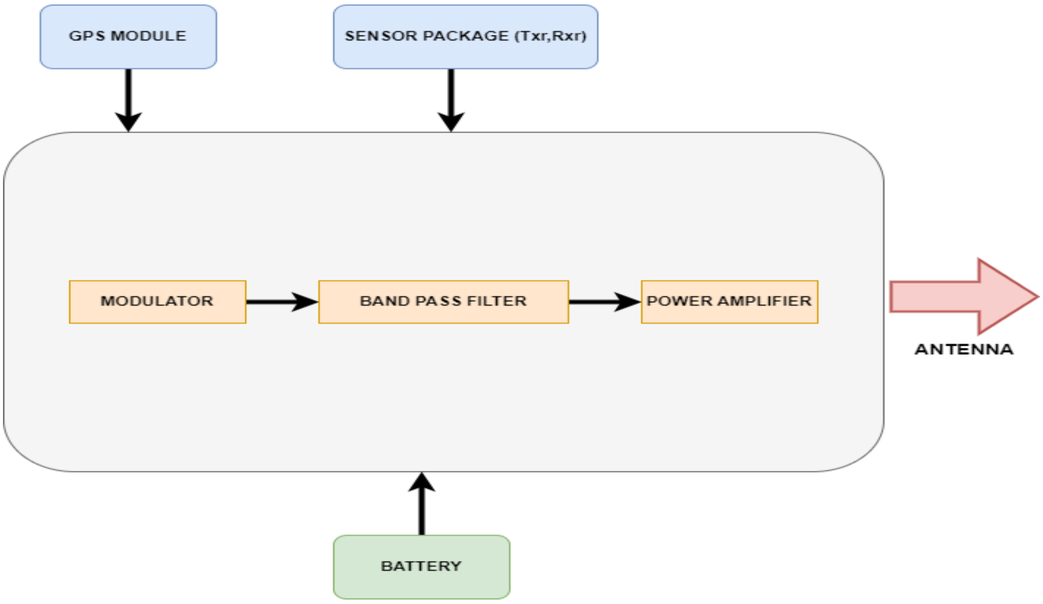

Fig 1 Radiosonde Block Diagram

Above figure 1, illustrates the signal processing flow within a radiosonde system, which includes a GPS module and a sensor package (transmitter and receiver). The GPS module and sensor package provide data inputs, which are fed into a modulator. The modulated signal then passes through a band-pass filter to remove unwanted frequencies and ensure that only the desired frequency range is transmitted. After filtering, the signal is amplified by a power amplifier to boost its strength before transmission. The entire process is powered by a battery, ensuring the continuous operation of the system. This setup ensures that the radiosonde effectively transmits accurate and strong signals containing atmospheric data.

From below figure 2, the internal architecture of a Radiosonde system, used for atmospheric data collection, is illustrated in a block diagram and divided into four main sections: Radiosonde Network, Backend Services, Data Services, and User Services. Each component and their interactions play a critical role in ensuring the system's efficiency and reliability. The Radiosonde Network comprises the Radiosonde Device, which is the hardware responsible for collecting atmospheric data. This device communicates with the backend services to transmit the collected data for further processing and storage. The Backend Services section includes several essential components. The Data Ingestion API serves as the entry point for the data transmitted by the Radiosonde Device. Once the data is received, it is passed on to the Data Processing Service. This service is responsible for cleaning, transforming, and preparing the data, ensuring it is suitable for storage and analysis. Moving on to the Data Services section, we find the Monitoring Service and Data Storage components. The Monitoring Service oversees the data processing pipeline and the overall health of the system, ensuring that all services are functioning correctly and that data is being processed accurately. The processed data is then stored in the Data Storage component, which can be accessed by various services for further use and analysis. The final section, User Services, includes several user-oriented components. The User Authentication service manages user credentials and permissions, ensuring that only authorized users can access the system. Once authenticated, users can interact with the system through the User Interface, which provides functionalities for data analysis. The Data Analytics Service offers tools and capabilities for analyzing the stored data, allowing users to derive insights from the atmospheric data collected by the Radiosonde Device. The interactions within this architecture are as follows: the Radiosonde Device sends data to the Data Ingestion API in the Backend Services. The Data Ingestion API forwards the data to the Data Processing Service, which processes the data and stores it in the Data Storage.

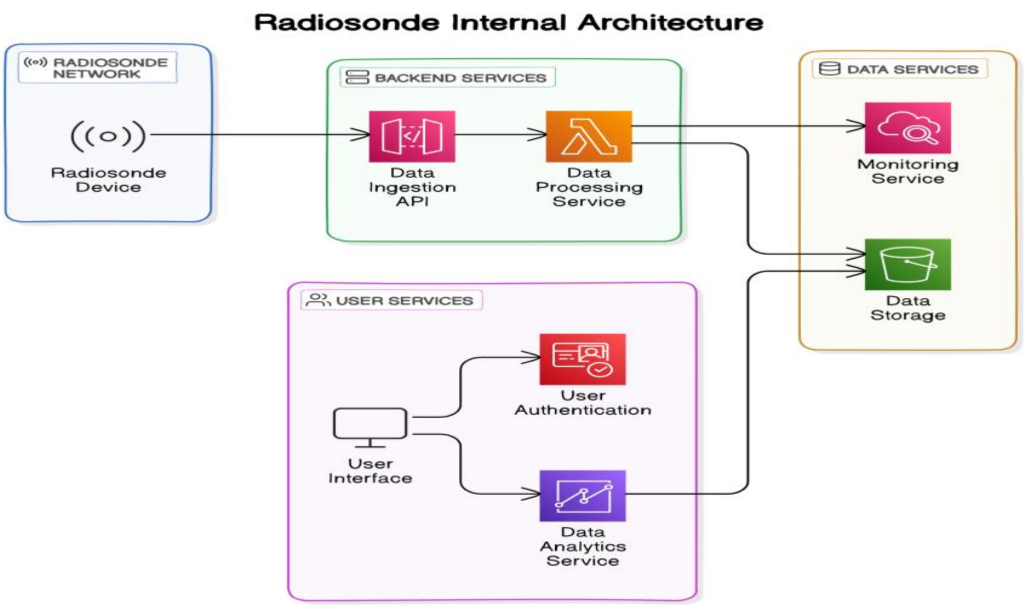

Fig 2 Radiosonde Internal Architecture

The Monitoring Service continuously monitors the Data Processing Service and the Data Storage to ensure system health. Users access the system via the User Interface, authenticate through the User Authentication service, and utilize the Data Analytics Service to analyze the stored data. Overall, this architecture ensures a seamless flow of data from collection to analysis, maintaining security and system health throughout the process.

4. Results and Discussions

The graph displays the relationship between altitude (in meters) and temperature (in degrees Celsius) for the period JJAS (June to September) in 2023 as shown in figure 3. The red line represents the temperature variation with increasing altitude. At approximately 5000 meters (5 kilometers) altitude, the temperature intersects with the zero degrees Celsius line. This intersection point indicates the altitude at which the temperature reaches freezing point. Below this altitude, temperatures are above zero degrees Celsius, while above this altitude, temperatures fall below freezing. The graph shows a general trend of decreasing temperature with increasing altitude, which is typical in atmospheric profiles, highlighting cooler conditions at higher elevations.

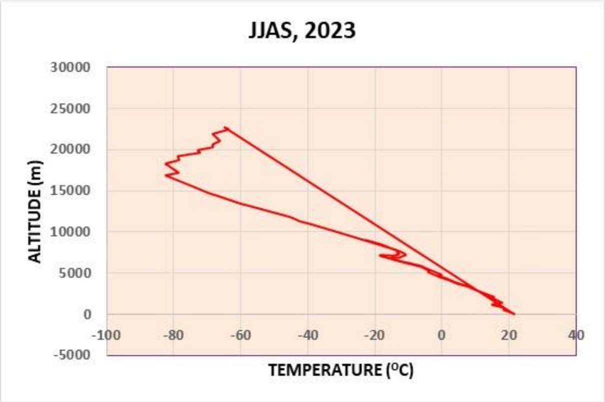

Fig 3 Bright Band Prediction for June, July, August and September, 2023

The Figure 4, shows the relationship between altitude (in meters) and temperature (in degrees Celsius) for the period of OND (October to December) in 2023. The black line represents the variation of temperature with increasing altitude. In this graph, the temperature intersects with the zero degrees Celsius line at approximately 5000 meters of altitude. This intersection point indicates the altitude at which the temperature reaches the freezing point. Below this altitude, temperatures are above zero degrees Celsius, while above this altitude, temperatures drop below the freezing point. The graph shows a general trend of decreasing temperature with increasing altitude, which is typical in atmospheric profiles, highlighting colder conditions at higher elevations.

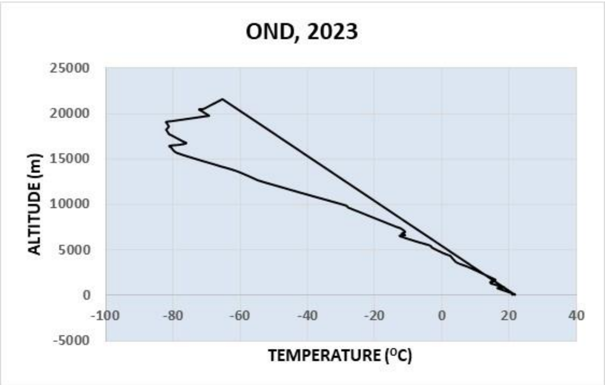

Fig 4 Bright Band Prediction for October, November and December, 2023

The graph depicts the relationship between altitude and temperature for the year 2024, showing an inverse correlation where temperature decreases as altitude increases. The temperature at sea level starts around 20°C and drops steadily with altitude as shown in figure 5. Notably, at approximately 5,000 meters, the temperature reaches 0°C, indicating the freezing point. As altitude continues to rise, temperatures fall more sharply, reaching as low as -80°C at around 20,000 meters. This trend is critical for understanding atmospheric conditions, especially in fields like aviation and meteorology.

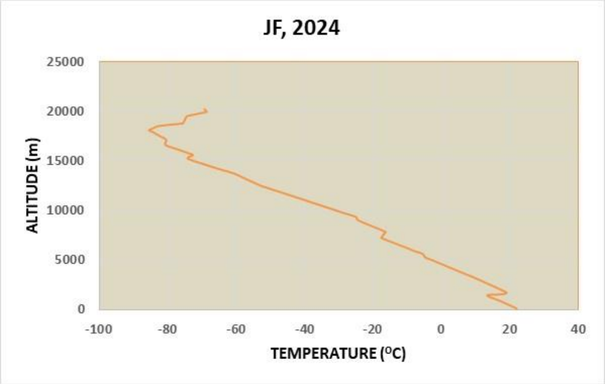

Fig 5 Bright Band Prediction for January and February, 2024

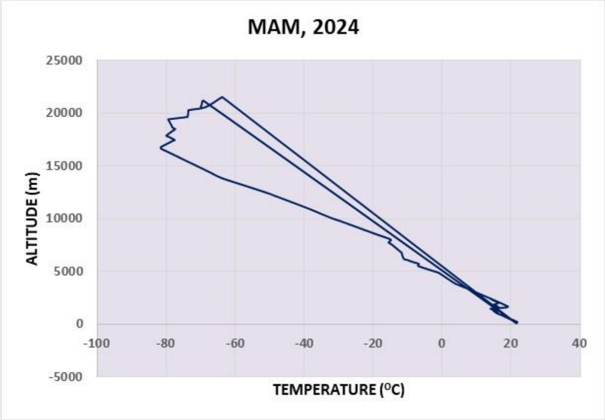

Fig 6 Bright Band Prediction for March, April and May, 2024

The graph as shown in Figure 6, illustrates the relationship between altitude and temperature for the period MAM 2024. As altitude increases, the temperature decreases, showing a clear inverse relationship. The temperature starts at around 20°C at lower altitudes and decreases sharply as altitude increases. The point where altitude meets temperature at 0°C is approximately at 4,800 meters. Beyond this point, the temperature continues to drop, reaching as low as -80°C at altitudes around 20,000 meters. This pattern demonstrates the typical lapse rate in the atmosphere where temperature decreases with an increase in altitude.

5. Conclusion

A constant recurrence of the bright band was found at an altitude of around 5000 meters (4800m to 5003m) in the study conducted utilizing RadioSonde RadioWind data at Visakhapatnam between June 2023 and May 2024. This phenomena suggests that there is a melting layer or bright band altering the properties of precipitation in the atmosphere. There could be consequences for the intensity and distribution of rainfall due to the altitude variations, which indicates susceptibility to seasonal and meteorological circumstances. Accurate hydrological modeling and regional weather forecasting depend on an understanding of the bright band dynamics at this particular altitude. In order to improve prediction skills and reduce uncertainties related to precipitation forecasting in the Visakhapatnam region, future research should concentrate on including more atmospheric characteristics and use sophisticated data assimilation algorithms.

Refrences

[1] Afullo, T. J., M. O. Adongo, T. Motsoela, and F. Molotsi. "A study of radio refractivity and super-refractivity in botswana." Transactions of the South African Institute of Electrical Engineers 90, no. 2 (1999): 61-68.

[2] Yi, Yang, Fan Yi, Fuchao Liu, Yun He, Yunpeng Zhang, and Changming Yu. "A prolonged and widespread thin mid-level liquid cloud layer as observed by ground-based lidars, radiosonde and space-borne instruments." Atmospheric Research 263 (2021): 105815.

[3] Fang Yuan, Zijiang Zhou, Jie Liao, Qinglei Li, "A quality control method for high-resolution radiosonde temperature and wind data" Atmospheric and Oceanic Science Letters, Volume 14, Issue 2, 2021, 100029, ISSN 1674-2834, https://doi.org/10.1016/j.aosl.2021.100029.

[4] Koner, Prabhat K., Andrew R. Harris, and Prasanjit Dash. "A deterministic method for profile retrievals from hyperspectral satellite measurements." IEEE Transactions on Geoscience and Remote Sensing 54, no. 10 (2016): 5657-5670.

[5] Feng, Peng, Rüdiger Haas, and Gunnar Elgered. "A Novel Tropospheric Error Formula for Ground-Based GNSS Interferometric Reflectometry." IEEE Transactions on Geoscience and Remote Sensing 61 (2023): 1-18.
[6] Mousa, Ashraf El-Kutb, Mostafa Rabah, Ahmed Saber, and Mohamed Zhran. "Analysis of spatial and temporal variation of precipitable water vapor using COSMIC radio occultation observations over Egypt." The Egyptian Journal of Remote Sensing and Space Science 25, no. 3 (2022): 751-764.
[7] Ahmed, Ibrahim Fouad, Mohamed Amin Abd El-Fatah, Ashraf El-Kutb Mousa, and Gamal El-Fiky. "Analysis of the differences between GPS radio occultation and radiosonde atmosphere profiles in Egypt." The Egyptian Journal of Remote Sensing and Space Science 25, no. 2 (2022): 491-500.
[8] Fu, Er-jiang, Ke-fei Zhang, Ka-ye Marion, Xiao-hua Xu, John Marshall, Anthony Rea, Gary Weymouth, and Yuriy Kuleshov. "Assessing COSMIC GPS radio occultation derived atmospheric parameters using Australian radiosonde network data." Procedia Earth and Planetary Science 1, no. 1 (2009): 1054-1059.
[9] Zhou, Qing, Yong Zhang, Junli Jin, Peng Yan, Mengyun Lou, Shanshan Lv, and Jiajia Mao. "Comparison of Atmospheric Boundary Layer Height Retrieved from Radiosonde and Groundbased Microwave Radiometer Measurements." In 2019 International Conference on Meteorology Observations (ICMO), pp. 1-4. IEEE, 2019.
[10] Gu, Jie, Yehui Zhang, Na Yang, and Rui Wang. "Comparisons in the global planetary boundary layer height obtained from COSMIC radio occultation, radiosonde, and reanalysis data" Atmospheric and Oceanic Science Letters 14, no. 2 (2021): 100018.
[11] India Meteorological Department (IMD). (2021). Overview of the IMD. Retrieved from IMD Website.
[12] World Meteorological Organization (WMO). (2017). Guide to Meteorological Instruments and Methods of Observation. WMO-No. 8. Retrieved from WMO Library.
[13] National Center for Medium Range Weather Forecasting (NCMRWF). (2020). Upper Air Observations. Retrieved from NCMRWF Website.
[14] Sikka, D. R., and Sulochana Gadgil. "On the maximum cloud zone and the ITCZ over Indian longitudes during the southwest monsoon." Monthly Weather Review 108, no. 11 (1980): 1840-1853.
[15] Maddikera, Krishna Reddy, Sarat K. Kotamraju, and K. Ch Sri Kavya. "Seasonal Rainfall Analysis of Vertically Pointing FMCW Micro Rain Radar." SN Computer Science 4, no. 5 (2023): 559.
[16] Maddikera, Krishna Reddy, Sarat K. Kotamraju, K. Ch Sri Kavya, and Bala Gangadhar Tilak Gande. "Radar reflectivity of micro rain radar(MRR2) at 16.44180 N, 80.620 E of India." International Journal of Integrated Engineering 14, no. 7 (2022): 162-185.
[17] Maddikera, Krishna Reddy, Sarat K. Kotamraju, K. Ch Sri Kavya, S. S. S. Kalyan, and Bala Gangadhar TilakGande. "Estimation of Melting Layerand Propagation Impairments Using Micro Rain Radar Dataat Coastal Locationof Andhra Pradesh."